COBEM 2021 26th International Congress of Mechanical Engineering
November 22-26, 2021, Virtual Congress, Brazil

COB-2021-0639
DETECTION AND IDENTIFICATION OF OVALIZATION FAULT IN HYDRODYNAMIC BEARINGS

Matheus Victor Inacio
Katia Lucchesi Cavalca
Gregory Bregion Daniel
School of Mechanical Engineering – UNICAMP. Rua Mendeleyev, 200 - Cidade Universitária, Campinas - SP, 13083-860
matheus.v.inacio@gmail.com; katia@fem.unicamp.br; gbdaniel@fem.unicamp.br;

Abstract. *Due to the crucial role that rotating machines have performed in the productive sector, there is an increasing demand on monitoring systems able to detect and identify early faults in order to avoid the sudden shutdowns and high maintenance costs. As one of the most critical sources of faults in rotating machines, hydrodynamic bearings require special attention, since they have a great influence on the dynamic behavior of the rotor. In this context, this paper aims to develop a method for the detection and identification of ovalization fault. For this, an ovalized bearing model was implemented by Finite Volume Method and introduced in a rotating system discretized by Finite Element Method, allowing simulating the dynamic response of the rotor under different ovalization faults. Several response-parameters are investigated to the proper identification of this kind of fault, such as the forward and backward components of the rotor response, the inclination angle and maximum and minimum radii of the shaft orbit. Based on these response-parameters, the ovalization fault can be identified in the bearings using numerical methods, in which the error functions were defined as the relative difference of the response-parameters obtained in the simulated and reference responses. Two different methods are evaluated in this paper, being the two-dimensional bisection and the Newton-Raphson, respectively, a dichotomous and a gradient method. The numerical simulations were performed considering different ovalization levels and angles, resulting in 16 cases of ovalized bearing. These 16 faulty cases were identified with both numerical methods, considering two different noise levels on the reference response, namely SNR of 12 db and 18 db. The results obtained in the simulations were quite satisfactory, since the fault identification was successfully accomplished. Regarding the search methods, the Newton-Raphson method performed faster identification, maintaining the same order of errors obtained in the two-dimensional bisection. Therefore, the findings obtained in this paper contribute to the improvement of faults monitoring systems applied in rotating machinery.*

Keywords: *Rotordynamics, Fault identification, Hydrodynamic Bearing, Ovalization Fault.*

1. INTRODUCTION

In the current scenario, rotating machines have a highly relevant role in the industry, given their large-scale use in this sector of the economy. Thus, it is essential to reduce downtime and maintenance costs of this kind of machine. However, the presence of faults and the absence of efficient monitoring systems impair an improved operation of these machines.

Hydrodynamic bearings are one of the rotating system components most susceptible to faults, being them very critical due to their importance on the dynamic response of the machine. For this reason, hydrodynamic bearings present a great demand for fault monitoring systems. However, due to the lack of in-depth knowledge about the influence of several types of hydrodynamic bearing faults on the dynamic response of the machine, the development of monitoring systems capable of identifying hydrodynamic bearing faults is still challenging.

Among the several types of faults related to the hydrodynamic bearings, ovalization is one of the most recurrent, being caused by non-symmetrical heating, manufacturing uncertainty and assembly problems, as stated by Takabi and Khonsari (2015). Regarding the bearing ovalization, Goenka and Booker (1983) obtained the equation for elliptical bearings through mathematical simplifications of the ellipse equation jointly with an analysis around the oil film thickness. This study was used as the basis for the ovalization analysis in radial hydrodynamic bearings.

Later, Crosby (1992) evaluated the influence of ovalization in hydrodynamic bearing, indicating that the maximum pressure increases as the ovalization amplitude becomes larger for constant ovalization angles. Silveira and Daniel (2019) also obtained important conclusions regarding bearing ovalization, concluding that the ovalization angle is determinant in the behavior of a planar connecting crank-rod.

In order to avoid downtime in production processes, methods of fault identification and detection in rotating machinery are increasingly being addressed in research topics, aiming to develop efficient tools of monitoring rotating systems. According to Silva (2018), there are two basic types of approaches used in the investigation of machine faults. The first is based on the historical data acquired from the machine, while the second approach is based on the physical knowledge

of the machine and its behavior. In this paper, the second approach is used, in which the fault identification is done using models of the real machines (model-based). According to Lees et al. (2009), this approach consists of developing mathematical models of the machines in order to generate estimated parameters and relate them to the parameters obtained from the measured responses. Thus, there is a need for robust models capable of simulating the physical effects of a real rotor, as well as typical fault conditions, allowing the detection and identification of different types of faults.

Alves et al. (2021) evaluated the dynamic behavior of a rotating system supported by magnetic bearings and hydrodynamic bearings with wear failure. Thus, the hydrodynamic bearing was modeled based on an improved wear fault model. Based on the experimental and numerical dynamic responses, it was concluded that the proposed wear model reproduced the experimental behavior with good accuracy. Moreover, the failure parameter identification tests showed very promising results.

Still exploring failures in hydrodynamic bearings, Alves et al. (2020) applied a numerical model to simulate ovalization failures in hydrodynamic bearings with the objective of generating a data set capable of assisting in the training of a neural network algorithm for the classification of the failure. The results showed that the machine learning algorithm represents a powerful tool capable of classifying failures. However, besides being necessary a large amount of data to guarantee a good accuracy, the proposed approach is limited, since it is only able to classify the ovalization failure in the labels or classes in which it was trained. Thus, there is a lack in the literature related to a method capable of identifying the parameters of faults for any ovalization level on the bearing, using only the vibrational response of the rotor as a reference signal.

Considering the promising results that the model-based identification has presented for bearings faults, this paper aims to developed a model-based technique to identify ovalization faults in hydrodynamic bearings. For this, an ovalization fault model was used to model the bearing, being it introduced in a rotating system discretized by Finite Elements Method. The vibration signals obtained by numerical model in the time domain were transformed to the directional coordinates in the frequency domain, thus obtaining the forward and backward components of the rotor's response as well as the parameters of the rotor's orbit shape inside the bearing. Thus, error functions can be formulated by calculating the relative difference of these parameters obtained from the simulated and reference responses. In this paper, the two-dimensional bisection and the classical Newton-Raphson method were applied in order to find the zeros of these error functions and estimate the variables of the hydrodynamic bearing ovalization. Finally, it is important to mention that the approach proposed in this paper contributes to a better understanding of the identification of ovalization failures in hydrodynamic bearings, thus allowing to expand and improve the performance of fault monitoring systems applied to rotating machines.

2. METHODOLOGY

This chapter presents the formulations and methods used in this work. Section 2.1 presents the numerical model of the hydrodynamic bearing with the ovalization fault. In following, section 2.2 describes the rotor model discretized by Finite Elements Method. Finally, section 2.3 presents the numerical root search methods used in the identification of the fault parameters.

2.1 Numerical model of the ovalized hydrodynamic bearing

Considering that the ovalization becomes the bearing profile as elliptical, an ovalization fault model was proposed by Silveira and Daniel (2019). In this model, Eq. (1) describes the oil film thickness for the ovalized bearing:

$$h(\theta) = Cr + e_x sen(\theta) - e_y cos(\theta) + kcos(2\theta - \alpha) \tag{1}$$

where the term $h(\theta)$ represents the oil film thickness as a function of θ, that is an angular coordinate referenced to the inertial axis Y, as showed in the schematic drawing of the ovalized bearing in Figure 1. Moreover, Cr represents the radial clearance, e_x and e_y the horizontal and vertical components of the shaft eccentricity inside the bearing and, finally, k and α are the magnitude and the angle of ovalization, respectively.

Once the oil film thickness equation is obtained, the pressure field can be solved numerically using the Finite Volume Method (FVM). Thus, the classical lubrication equation described by Reynolds (1886) is considered, as described in Eq. (2).

$$\frac{\partial}{\partial x}\left(h^3 \frac{\partial p}{\partial x}\right) + \frac{\partial}{\partial z}\left(h^3 \frac{\partial p}{\partial z}\right) = 6\mu U \frac{dh}{dx} + 12\mu \frac{dh}{dt} \tag{2}$$

where p represents the pressure field, μ the dynamic viscosity of the lubricating oil, U the linear velocity on the shaft surface, and (X, Z) the coordinates of the bearing domain. After determining the pressure distribution on the bearing, the hydrodynamic forces of the ovalized bearings can be calculated integrating the pressure field on the bearing domain.

Since the shaft vibration inside the bearing presents small amplitude, the hydrodynamic forces can then be linearized around the static equilibrium position, thus obtaining the equivalent coefficients of stiffness K_{ij} and of damping C_{ij}, as proposed by Lund (1987).

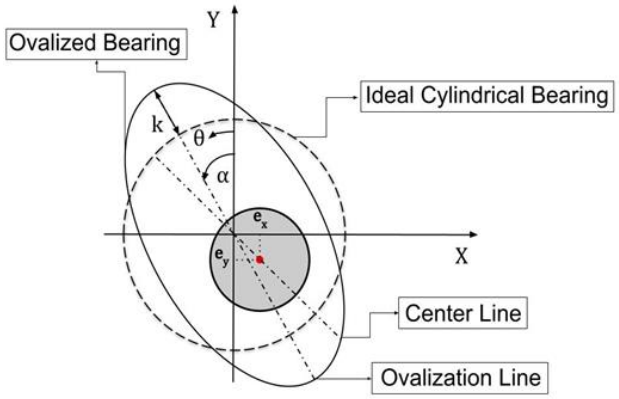

Figure 1. Ovalized bearing schematic drawing

These equivalent coefficients can be calculated by partial derivatives of the hydrodynamic forces with respect to shaft displacement and velocity. Moreover, such derivatives can be approximated by varying the forces as a function of small perturbations of displacement and velocity around the equilibrium position.

$$F_{h,x} = F_{h,x0} + K_{xx.}(e_x - e_{x0}) + K_{xy}.\left(e_y - e_{y0}\right) + C_{xx}.\dot{e_x} + C_{xy}.\dot{e_y} \tag{3}$$

$$F_{h,y} = F_{h,y0} + K_{yx}.(e_x - e_{x0}) + K_{yy}.\left(e_y - e_{y0}\right) + C_{yx}.\dot{e_x} + C_{yy}.\dot{e_y}$$

where $F_{h,x}$ and $F_{h,y}$ are the resultant hydrodynamic forces in the X and Y direction of the inertial system, e and $\dot{e}$ are the position and velocity of the center of the shaft, e_{x0} and e_{y0} represents the static equilibrium position inside the bearing.

In order to obtain the dynamic response of the rotor considering the influence of the ovalized bearings, the hydrodynamic forces described in Eq. (3) should be inserted into the equation of motion of the rotating system via the external force vector.

2.2 Numerical model of the rotating system

In this paper, the rotating system is modeled by Finite Element Method (FEM), being composed of cylindrical Timoshenko beam elements and rigid disk element. In this model, each node has four degrees of freedom, being two translational in the X and Y directions and two angular around the X and Y axes (lateral vibration).

From the FEM it is possible to obtain the global matrices of mass ($[M_G]$), stiffness ($[K_G]$), gyroscopic ($[G_G]$) and damping ($[C_G]$), in which it is assumed as proportional to mass and stiffness, similar to proposed by Ramos and Daniel (2020). In addition, the vector of external forces ($\{F_G\}$) is also obtained, being composed of the rotor weight, hydrodynamic forces of the bearings (F_h) and the unbalance force that is responsible to excite the rotor. The global equation of motion of the rotating system is presented in Eq. (4):

$$[M_G]\{\ddot{q}\} + ([C_G] + \Omega[G_G])\{\dot{q}\} + [K_G]\{q\} = \{F_G\} \tag{4}$$

Integrating the Eq. (4) in relation to time, the dynamic response of the rotor is obtained.

The response parameters used in the identification of the ovalization fault are calculated transforming the permanent temporal response to the directional coordinates (f, b) in the frequency domain. For this, firstly the permanent temporal response is transformed to the frequency domain, obtaining the FullSpectrum of the response in the physical coordinates (X, Y). Then, a change of coordinates is applied, transforming the physics (X, Y) to the directional coordinates (f, b), as proposed by Mendes (2016). Eq. (5) presents this coordinates transformation:

$$\begin{Bmatrix} f \\ \bar{b} \end{Bmatrix} = \begin{bmatrix} 1/2 & i/2 \\ 1/2 & -i/2 \end{bmatrix} \begin{Bmatrix} X \\ Y \end{Bmatrix} \tag{5}$$

where X is the physic coordinate in the inertial reference system, Y is the physic coordinate in the inertial reference system f is the forward coordinate, b is the backward coordinate and i is the imaginary unit ($i = \sqrt{-1}$).

Amplitudes at frequency 1x (forward) and -1x (backward) are used as parameters for identifying the ovalization fault, since the system response is predominantly synchronous with rotation due to the unbalance excitation and the linearized hydrodynamic forces.

After obtaining the parameters of the directional coordinates (forward and backward amplitudes), the parameters of the orbit shape of the shaft inside the bearing are calculated for identifying the ovalization fault. The orbit shape is composed of the maximum radius, minimum radius and inclination angle, being also calculated using the amplitudes and phases of the directional coordinates at 1x and -1x frequencies as shown in Figure 2.

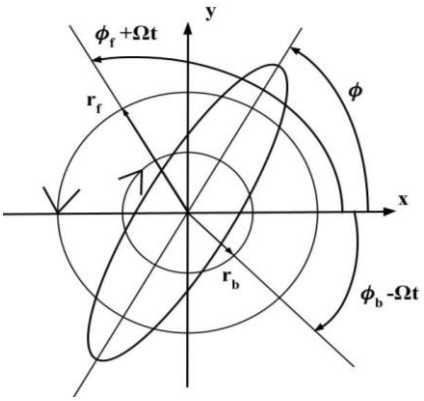

Figure 2. Representation of the relationship of the orbit shape to the directional coordinates

According to Lee (1993), the maximum radius, minimum radius and inclination angle can be obtained as presented in Eq. (6):

$$R_{max} = |rf| + |rb| \tag{6}$$

$$R_{min} = ||rf| - |rb||$$

$$\phi = \frac{\phi_f + \phi_b}{2}$$

where rf and ϕ_f are the amplitude and phase at 1x frequency (forward), respectively; rb and ϕ_b are the amplitude and phase at - 1x frequency (backward), respectively; R_{max}, R_{min}, and ϕ are the maximum radius, minimum radius and inclination angle of the shaft orbit inside the bearing, respectively.

2.3 Numerical methods for identification of ovalization faults

Model-based techniques for fault identification consist of comparing the responses obtained from mathematical models with the physical responses of the machines during the operating condition, in order to diagnose possible faults and, if necessary, to identify the fault parameters that affect the dynamic behavior of the rotor. To perform this comparison between responses, numerical methods can be used to search the roots of error functions.

The error functions used in the ovalization fault identification process are obtained based on parameters of the dynamic response of the rotor, namely: 1x (forward) and -1x (backward) amplitudes, maximum radius, minimum radius and inclination angle of the shaft orbit inside the bearing. These error functions are calculated by the relative difference between the reference response parameter and the simulated response parameter, being obtained based on the ovalization variables (k,α) as describes in Eq. (7).

$$f_{pt}(k, \alpha) = \frac{pt(k,\alpha) - pt_{ref}}{pt_{ref}} \tag{7}$$

where f_{pt} is the error function of the parameter pt of the rotor dynamic response with respect to the reference parameter pt_{ref}.

In this paper, two different numerical methods are used to search the roots of these error functions. The first is the two-dimensional bisection that is a dichotomous method and the second is Newton-Raphson that is a gradient method.

2.3.1 Two-dimensional bisection method

According to Menezes (2015), the two-dimensional bisection method is a generalization of the one-dimensional bisection method, in which an initial interval is divided in half and the side that has the zero of the function is determined, making this side the interval for the next iteration. However, for two-dimensional case, a primary rectangle is firstly formed by defining the initial intervals for each of the variables. Then, each dimension is divided in half, splitting the initial rectangle into four smaller rectangles of congruent dimensions. Once the four rectangles are obtained, the value of the error function is calculated in each of the vertices of the rectangles, in order to identify the rectangle with the zero of the function.

In applying this method, the error functions of the five parameters of the dynamic response were used. Therefore, those rectangles that present equal signs (positive or negative) in all four vertices for at least one of the error functions are eliminated from the search, while the others continue to be subdivided into new four rectangles, repeating the same procedure at each iteration. However, if all rectangles are eliminated before to reach the convergence, the rectangles elimination process is redone, increasing by one the number of error functions with equal signs at the vertices needed for elimination of the rectangles. An example of the quadrant elimination process that occurs only after the first iteration is shown in Figure 3. The "X" inside the quadrants indicates their elimination, while those not eliminated are further subdivided as described by the bisection process.

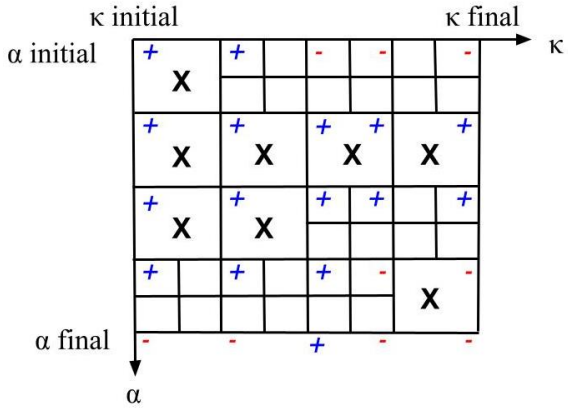

Figure 3. Schematic representation of the rectangles elimination process of the two-dimensional bisection method

For the ovalization identification, the stopping criterion is based on the ratio between the edge size and the centroid of the variable k of each rectangle. Thus, the algorithm is stopped when all rectangles have this ratio (edge/centroid) less than 1%. This ensures that the rectangle is sufficiently small in relation to the ovalization magnitude, making the solution more robust and reliable. In some cases, there is more than one rectangle as solution after the convergence. In order to determine which of these rectangles contain the best solution, the absolute mean value of the forward and backward error functions (the parameters most sensitive to ovalization) are summed for each rectangle. In this way, the rectangle with the smallest value represents the possible solution, which in this case refers to the centroid of the rectangle.

2.3.2 Newton-Raphson Method

Despite the high robustness, dichotomous methods have the disadvantage to be costly methods due to the need for a large number of iterations, as well as needing a comprehensive domain to ensure that the search is performed in the correct region. Thus, gradient search methods are a very viable alternative, since they can converge with fewer steps if a good initial estimate is made (Menezes, 2015).

Among the gradient search methods, the Newton-Raphson method is commonly applied to solve nonlinear and transcendental equations. The great advantage of this method is its speed of convergence, characterized by being locally quadratic (Sassi, 2010).

The Newton-Raphson method applied for the identification of the ovalization fault uses the error functions of forward amplitude, backward amplitude and orbit inclination angle. As these functions are discrete, their derivatives for the Jacobian are approximated by the Finite Differences Method (FDM). The formulation related to Newton-Raphson method is shown in Eq. (8):

$$\{X\}^{(i+1)} = \{X\}^{(i)} - [J(\{X\}^{(i)})]^{-1}\{f(\{X\}^{(i)})\} \tag{8}$$

where $\{X\}^{(i)}$ is the vector with the k and α parameters of the iteration i, $\{X\}^{(i+1)}$ is the vector with the updated k and α parameters of the iteration $i+1$, $\{f(\{X\}^{(i)})\}$ is the vector of the error functions of the iteration i and $[J(\{X\}^{(i)})]$ is the Jacobian matrix, being the partial derivatives of the error functions related to k and α parameters of the iteration i.

The initial estimates of the k and α parameters in the vector $\{X\}^{(0)}$ are very important for the converge. For this reason, the multi-start strategy is used for the Newton-Raphson method, where nine initial estimates are considered and equally spaced in the search domain. Initially, the quadratic norms of the vector $\{f(\{X\}^{(0)})\}$ are calculated for these nine initial guesses, in which the search process starts from the guess with the lowest norm. If the stopping criterion is not reached until 20 iterations, a new search process is restarted from the guess with the second lowest norm.

Finally, this numerical procedure is stopped when the modulus of the error functions is lower than $7.5.10^{-3}$ and the k and α parameters have a variation smaller than $7.5.10^{-2}$ and $7.5.10^{-1}$, respectively.

3. NUMERICAL RESULTS

This section presents the numerical results of the ovalization faults identification tests, considering the numerical methods described in subsection 2.3. The rotating system used in the numerical tests consists of a rotor supported by hydrodynamic bearings, whose rotational speed is 32 Hz. This rotor is modeled by Finite Element Method (FEM), as shown in Figure 4.

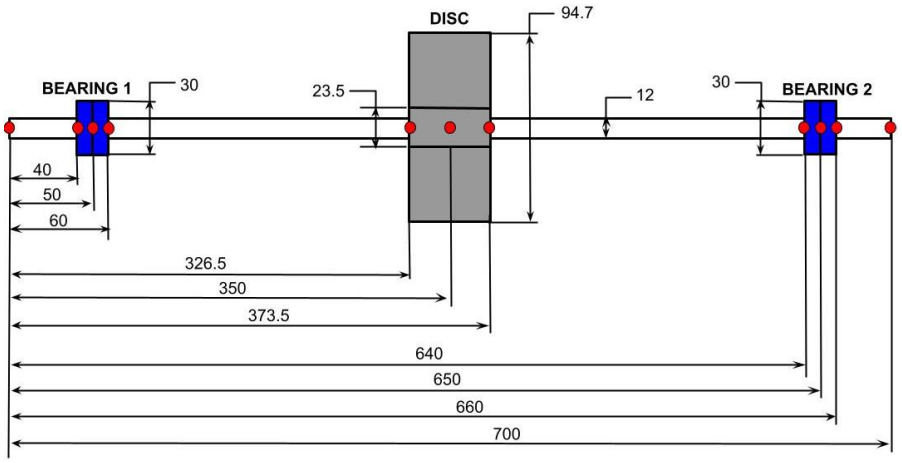

Figure 4. Rotating system modeled by FEM (Dimensions in mm)

Table 1 presents the rotor parameters used in the mathematical modeling, while Table 2 presents the parameters used in the bearing model.

Table 1. Rotor parameters

Parameters	Values
Density, kg/m^3	7850
Young Modulus, GPa	200
Unbalance Mass, kg	$1.7.10^{-3}$
Unbalance Eccentricity, m	$3.7.10^{-2}$
Inertia Proportionality Constant	0
Stiffness Proportionality Constant	1.10^{-4}

Table 2. Bearing and lubricant oil parameters

Parameters	Values
Diameter, m	3.10^{-2}
Width, m	2.10^{-2}
Radial Clearance, m	9.10^{-5}
Oil Dynamic Viscosity, Pa.s	5.10^{-2}
Discretization Mesh (FVM)	150x150
Load, N	16.58

In order to evaluate the proposed approach for identification of the ovalization faults parameters, the methods are applied to different 16 cases, being distributed in an initial search domain with k varying into 0.0-15.0% of radial clearance (Cr) and α varying into 0-90°.

In this paper, the reference responses used for ovalization identification are obtained from numerical simulations, being it contaminated with white Gaussian noise in order to represent experimental measurements. The signal-to-noise ratio (SNR) values of the white Gaussian noise are of 12 dB and 18 dB. As an example, Figure 5 shows the influence of the noise on the reference dynamic response, obtained from the shaft displacement signal in X on the bearing 1.

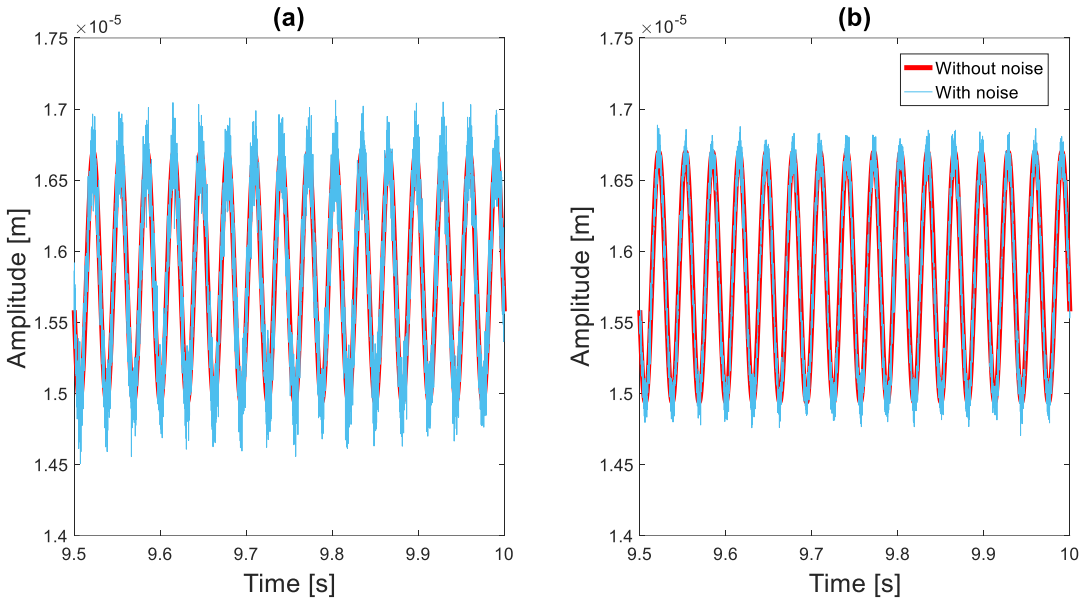

Figure 5. Shaft displacement on the bearing 1 with ovalization $k = 3\%\ Cr$ e $\alpha = 60°$: (a) Signal without noise and with noise SNR=12 dB, (b) Signal without noise and with noise SNR=18 dB

3.1 Two-dimensional bisection method applied to the identification of ovalization fault

This subsection evaluates the robustness and efficiency of the two-dimensional bisection method for identification of the ovalization faults parameters in hydrodynamic bearings. The identification accuracy is evaluated based on relative errors of the parameters k and α identified in relation to the parameters adopted for the tests. The computational cost of the identification is analyzed through the time spent on the search process.

Table 3 presents the results of the ovalization identification for the 16 cases performed by two-dimensional bisection.

Table 3. Results of the two-dimensional bisection method applied to the identification of ovalization

		Signal-to-Noise Ratio (SNR) of 18 dB			**Signal-to-Noise Ratio (SNR) of 12 dB**		
Case	**[k(%); α(°)] adopted**	**[k(%); α(°)] identified**	**Error (%)**	**Time (h)**	**[k(%); α(°)] identified**	**Error (%)**	**Time (h)**
1	[3; 0]	[3.01; 0.44]	[0.33; -]	11.02	[3.03; 0.44]	[1.00; -]	11.95
2	[3; 30]	[3.01; 29.62]	[0.33; -1.27]	18.35	[3.03; 29.44]	[1.00; -1.87]	19.66
3	[3; 60]	[2.98; 61.44]	[-0.67; 2.40]	39.98	[2.84; 56.51]	[-5.33; -5.82]	46.57
4	[3; 90]	[2.81; 87.28]	[-6.33; -3.02]	24.94	[2.81; 87.28]	[-6.33; -3.02]	25.28
5	[6; 0]	[5.91; 1.58]	[-1.50; -]	10.17	[5.91; 2.29]	[-1.50; -]	13.05
6	[6; 30]	[5.97; 30.06]	[-0.50; 0.20]	13.37	[6.19; 30.76]	[3.17; 2.53]	9.98
7	[6; 60]	[6.08; 57.48]	[1.33; -4.20]	12.42	[5.85; 59.59]	[-2.50; -0.68]	13.49
8	[6; 90]	[6.08; 89.47]	[1.33; -0.59]	10.38	[6.14; 89.12]	[2.33; -0.98]	18.16
9	[9; 0]	[9.02; 0.18]	[0.22; -]	9.56	[9.08; 0.18]	[0.89; -]	10.79
10	[9; 30]	[8.97; 30.06]	[-0.33; 0.20]	9.31	[9.02; 29.36]	[0.22; -2.13]	10.12
11	[9; 60]	[9.02; 59.59]	[0.22; -0.68]	8.90	[8.85; 59.94]	[-1.67; -0.10]	10.08
12	[9; 90]	[8.97; 88.77]	[-0.33; -1.37]	9.47	[8.97; 88.42]	[-0.33; -1.76]	12.38
13	[12; 0]	[11.77; 1.76]	[-1.92; -]	11.37	[10.50; 0.18]	[-12.50; -]	11.08
14	[12; 30]	[12.00; 30.59]	[0.00; 1.97]	8.65	[12.22; 29.18]	[1.83; -2.73]	10.97
15	[12; 60]	[12.00; 61.52]	[0.00; 2.53]	8.97	[12.00; 60.12]	[0.00; 0.20]	8.76
16	[12; 90]	[12.11; 89.65]	[0.92; -0.39]	9.02	[12.11; 89.65]	[0.92; -0.39]	9.44
Mean	-	-	[1.02; 1.57]	13.49	-	[2.63; 1.85]	15.11

According to Table 3, it is possible to verify that the parameters are properly identified in most of the cases. Moreover, all average errors are below 5% for both SNR values, although the cases with SNR=12 dB presented higher errors, which is expected since the reference signal is more contaminated. Therefore, it can be seen that the results obtained are very promising, and it can be concluded that the dichotomous search algorithm developed for the ovalization identification of hydrodynamic bearings proved to be accurate and robust.

It can also be seen that as the bearing deformation increases (k increases), generally the search time decreases considerably, indicating that the efficiency of the method increases in these cases. This behavior occurs because the fault signatures in the rotor response signals are more significative for more critical fault conditions.

The cases 4 and 13 showed the most critical identifications in terms of accuracy for SNR of 18 and 12 dB, respectively. Figure 6 shows the search process performed by the two-dimensional bisection method for these two specific cases.

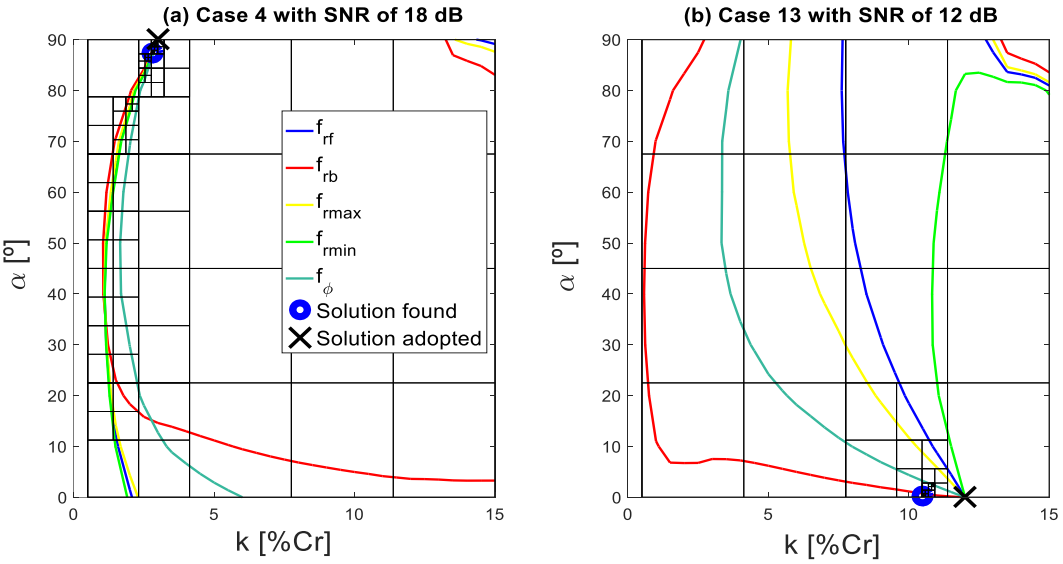

Figure 6. Search process performed by the two-dimensional bisection method: (a) Case 4 with SNR of 18 dB; (b) Case 13 with SNR of 12 dB

Analyzing Figure 6, one can see that for both cases the search process performed by the bisection method works as proposed, where the region containing the solution, given by the intersection of the level curves of the roots of the error functions, is subdivided into smaller quadrants, while the rest of the quadrants are eliminated until a numerical solution is obtained.

The solution of case 4 for the reference signal with 18 dB noise showed percentage errors of -6.33% and -3.02% for the ovalization variables k and α, while the identification of case 13, where the reference signal had 12 dB noise, showed -12.50% for variable k. This justifies the greater distance between the adopted solution and the one found in Figure 6b.

3.2 Newton-Raphson method applied to the identification of ovalization failure

Similarly to bisection method, the efficiency and robustness of the Newton-Raphson method applied to the ovalization fault identification is then evaluated in this subsection. Table 4 presents the result of identifying the ovalization failure parameters of the 16 test cases for the noise levels of 18 and 12 dB by applying Newton-Raphson.

According to Table 4, it can be seen that some cases of ovalization with α = 90º presented negative values for the identified parameter, since that both angles (90º and -90º) generate the same shapes of ovalization. In addition, it is noted that the Newton-Raphson method also showed good accuracy for the fault parameters identification, although the relative errors of the α parameter were greater than obtained by two-dimensional bisection method, especially for signals with SNR of 12 dB that resulted an average error of identification of 5.24%. As previously mentioned, these cases with SNR of 12 dB represents very noisy reference response signals, making it difficult to identify the fault parameters.

Although some cases demanded high search times due to non-convergence of the first initial estimates on the multi-start strategy, such as cases 1 and 4 with SNR of 18 dB and cases 4, 5 and 7 with SNR of 12 dB, the most of the fault identification cases had presented search times below 10 hours. Therefore, it can be seen that the Newton-Raphson method has a lower computational cost compared to two-dimensional bisection method, with an average search time of 9.15 and 7.23 hours for the cases with SNR of 18 and 12 dB, respectively.

Based on the results presented in Table 4, the cases 3 and 6 are the most critical identifications for SNR of 18 and 12 dB, respectively. Thus, Figure 8 shows the search process performed by the Newton-Raphson method for these two specific cases.

Table 4. Results of the Newton-Raphson method applied to the identification of ovalization

		Signal-to-Noise Ratio (SNR) of 18 dB			Signal-to-Noise Ratio (SNR) of 12 dB		
Case	**[*k*(%); α(°)] adopted**	**[*k*(%); α(°)] found**	**Error (%)**	**Time (h)**	**[*k*(%); α(°)] found**	**Error (%)**	**Time (h)**
1	[3; 0]	[2.97; -0.50]	[-1.00; -]	35.32	[3.29; -0.25]	[9.67; -]	9.25
2	[3; 30]	[3.05; 29.37]	[1.67; -2.10]	3.97	[3.06; 29.29]	[2.00; -2.37]	4.65
3	[3; 60]	[3.00; 53.90]	[0.00; -10.17]	5.20	[3.01; 53.34]	[0.33; -11.10]	4.51
4	[3; 90]	[3.03; -89.49]	[1.00; -0.57]	47.47	[3.26; -87.21]	[8.66; -3.10]	14.59
5	[6; 0]	[5.89; 0.04]	[-1.83; -]	4.48	[5.85; -0.26]	[-2.50; -]	23.93
6	[6; 30]	[5.86; 31.05]	[-2.33; 3.50]	3.68	[5.53; 35.46]	[-7.83; 18.20]	4.60
7	[6; 60]	[6.02; 59.90]	[0.33; -0.17]	5.81	[5.85; 64.98]	[-2.50; 8.30]	16.68
8	[6; 90]	[5.98; 90.28]	[-0.33; 0.31]	4.20	[6.03; 81.83]	[0.50; -9.08]	2.54
9	[9; 0]	[8.62; 1.19]	[-4.22; -]	3.37	[8.84; 0.51]	[-1.78; -]	4.53
10	[9; 30]	[8.86; 31.42]	[-1.56; 4.73]	3.71	[8.95; 30.26]	[-0.56; 0.87]	3.05
11	[9; 60]	[8.98; 59.82]	[-0.22; -0.30]	3.93	[9.11; 62.06]	[1.22; 3.43]	3.34
12	[9; 90]	[8.96; -89.94]	[-0.44; -0.07]	9.40	[8.92; 90.13]	[-0.89; 0.14]	5.60
13	[12; 0]	[11.99; -0.02]	[-0.08; -]	3.56	[11.82; 0.09]	[-1.50; -]	6.42
14	[12; 30]	[12.00; 30.00]	[0.00; 0.00]	3.73	[12.26; 28.33]	[2.17; -5.57]	3.05
15	[12; 60]	[11.98; 61.06]	[-0.17; 1.77]	4.72	[11.93; 60.39]	[-0.58; 0.65]	5.65
16	[12; 90]	[11.99; 89.87]	[-0.08; -0.14]	3.84	[12.01; 90.06]	[0.08; 0.07]	3.35
Mean	-	-	[0.96; 1.99]	9.15	-	[2.67; 5.24]	7.23

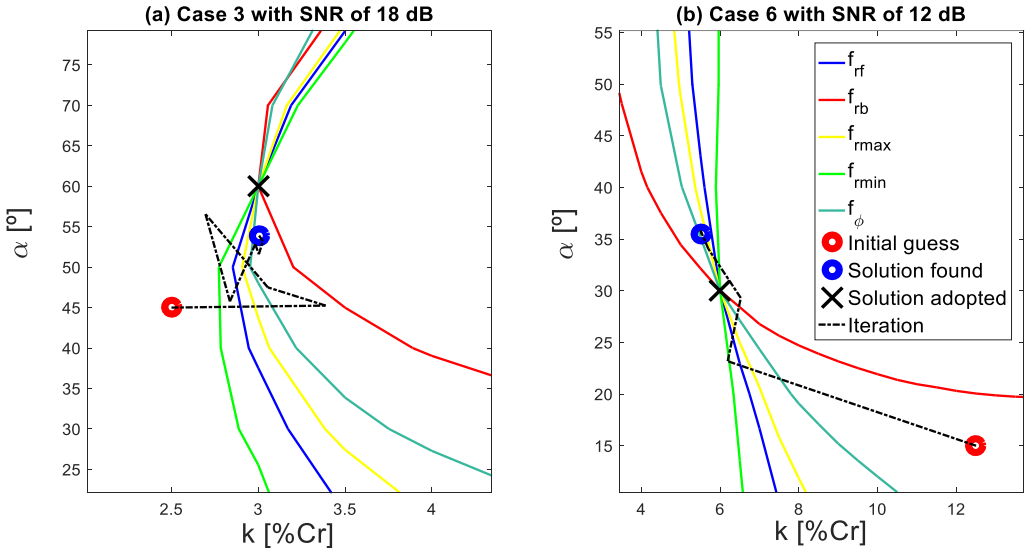

Figure 8. Search process performed by the Newton-Raphson method: (a) Case 3 with SNR of 18 dB; (b) Case 6 with SNR of 12 dB

Figure 8 shows the search process performed by Newton-Raphson method for the cases that presented the highest relative errors with SNR of 18 and 12 dB. As can be observed, the method worked correctly, approaching the adopted solution by few iterations from a close initial estimate.

Therefore, this work has developed a method capable of identifying the parameters of faults for different ovalization level on the bearing using only the vibrational response of the rotor. Moreover, it is possible to verify that this method presents a good performance, since the accuracy obtained in the numerical tests is slightly larger to that presented in the literature for the classification of specifics ovalization faults (Alves et al., 2020), besides to not require a large database in advance and not has training costs for machine learning techniques. Thus, this work complements the scientific development presented in the literature, providing more contributions to the field of fault identification applied to the rotating machines.

4. CONCLUSION

Based on analyses performed in this paper, it was possible to conclude that the methods proposed for the identification of ovalization faults are very promising, due to their significant efficiency and robustness obtained for different faulty cases and noisy signals. The identified parameters related to the ovalization fault presented low average relative errors, even with reference signals contaminated by high levels of noise (SRN=12 dB). Furthermore, it was verified that the ovalization parameters identification tends to be easier as the ovalization magnitude increases, since the fault signatures become more critical and relevant in the vibration signals.

The two-dimensional bisection method provided more accurate results in comparison to Newton-Raphson method, especially on the reference signal with SNR of 12 dB. On the other hand, the Newton-Raphson method is more efficient, since it has a lower computational cost.

In general way, this paper shows that the methods proposed for the identification of ovalization fault provide promising results, indicating a proper use for application in fault diagnosis and monitoring of rotating machinery. Thus, these advances aim to contribute on the adequately maintenance planning and unexpected downtime reduction in the production system, avoiding economic losses and helping to prevent accidents.

5. ACKNOWLEDGEMENTS

The authors thank the São Paulo Research Foundation (FAPESP) and the University of Campinas (UNICAMP) for financial support and infrastructural. Special thanks to Marcus Vinícius Medeiros Oliveira and Eduardo Carneiro Pereira for their help related to numerical root search methods and rotor modeling.

6. REFERENCES

Alves, D.S., Daniel, G.B., de Castro, H.F., Machado, T.H., Cavalca, K.L., Gecgel, O., Ekwaro-Osire, S., 2020. "Uncertainty quantification in deep convolutional neural network diagnostics of journal bearings with ovalization fault". Mechanism and Machine Theory 149 (2020), doi: 10.1016/j.mechmachtheory.2020.103835.

Alves, D.S., Fieux, G., Machado, T.H., Keogh, P.S., Cavalca, K.L., 2021. "A parametric model to identify hydrodynamic bearing wear at a single rotating speed". Tribol. Int. 153 (2021), doi: 10.1016/j.triboint.2020.106640.

Crosby, W.A., 1992. "An investigation of the performance of a journal bearing with a slightly irregular bore", Tribol. Int. 25 (1992) 199–204, doi:10.1016/ 0301- 679X(92)90049-S.

Goenka, P.K., Booker, J.F., 1983. "Effect of surface ellipticity on dynamically loaded cylindrical bearings", J. Lubr. Technol, 105 (1983), pp. 1-9, doi: 10.1115/1.3254535.

Lee, C.W., 1993. "Vibration Analysis of Rotors". 1.ed. Dordrecht /Boston/London: Kluwer Academic Publishers, pp. 44-45.

Lees, A.W., Sinha, J.K., Friswell, M.I., 2009. "Model-based identification of rotating machines", Mech. Syst. Signal Process., v. 23, p. 1884-1893.

Lund, J.W., 1987. "Review of the concept of dynamic coefficients for fluid film journal bearings", J. Tribol. 109 (1987) 37–41, doi: 10.1115/1.3261324.

Mendes, R.U., 2016. *Experimental Validation of a Model for Identification of Failure Parameters by Wear in Lubricated Bearings* (in Portuguese). Doctor's Thesis, Post-Graduate Program in Mechanical Engineering, State University of Campinas, Campinas, Brazil.

Menezes, M., 2015. *Numerical Calculus* (in Portuguese). Laureate- International Universities, pp.22-26.

Ramos, D. J., Daniel, G. B., 2020. "Evaluation of bearing's cavitation effects on the rotor dynamic behavior". Applied Mathematical Modelling 77 (2020), doi: 10.1016/j.apm.2019.07.026.

Reynolds, O., 1886. "On the theory of lubrication and its application to Mr. Beauchamp Tower's experiments, including an experimental determination of the viscosity of olive oil", Proc. Royal Soc. Lond., 40, pp. 191-203.

Sassi, C.A., 2010. *On the performance of Quasi-Newton methods and applications* (in Portuguese). Master's Thesis, Post-Graduate Program in Institute for Mathematics, Statistics and Scientific Computing, State University of Campinas, Campinas, Brazil.

Silva, M.C., 2018. *Artificial Intelligence Methods for Diagnosis of Rotating Machinery Defects* (in Portuguese). Graduation Work, Graduate Program in Electrical and Electronics Engineering, Federal University of Santa Catarina, Florianópolis, Brazil.

Silveira, A.R.G., Daniel, G.B., 2019. "Influence of bearing ovalization in the dynamic of a planar slider-crank mechanism". Applied Mathematical Modelling, 66, pp 175-194.

Takabi, J., Khonsari, M.M., 2015. "On the thermally-induced seizure in bearings: a review". Tribol. Int. 91 (2015) 118–130, doi: 10.1016/j.triboint.2015.05.030.

7. RESPONSIBILITY NOTICE

The authors are the only responsible for the printed material included in this paper.